Identification of Regulatory Phosphorylation Sites in a Cell Volume–and Ste20 Kinase–dependent ClC Anion Channel

Rebecca A. Falin,[1] Rebecca Morrison,[1] Amy-Joan L. Ham,[2] and Kevin Strange[1]

[1]Departments of Anesthesiology and Molecular Physiology and Biophysics, and [2]Department of Biochemistry, Vanderbilt University Medical Center, Nashville, TN 37232

Changes in phosphorylation regulate the activity of various ClC anion transport proteins. However, the physiological context under which such regulation occurs and the signaling cascades that mediate phosphorylation are poorly understood. We have exploited the genetic model organism *Caenorhabditis elegans* to characterize ClC regulatory mechanisms and signaling networks. CLH-3b is a ClC anion channel that is expressed in the worm oocyte and excretory cell. Channel activation occurs in response to oocyte meiotic maturation and swelling via serine/threonine dephosphorylation mediated by the type I phosphatases GLC-7α and GLC-7β. A Ste20 kinase, germinal center kinase (GCK)-3, binds to the cytoplasmic C terminus of CLH-3b and inhibits channel activity in a phosphorylation-dependent manner. Analysis of hyperpolarization-induced activation kinetics suggests that phosphorylation may inhibit the ClC fast gating mechanism. GCK-3 is an ortholog of mammalian SPAK and OSR1, kinases that bind to, phosphorylate, and regulate the cell volume–dependent activity of mammalian cation-Cl^- cotransporters. Using mass spectrometry and patch clamp electrophysiology, we demonstrate here that CLH-3b is a target of regulatory phosphorylation. Concomitant phosphorylation of S742 and S747, which are located 70 and 75 amino acids downstream from the GCK-3 binding site, are required for kinase-mediated channel inhibition. In contrast, swelling-induced channel activation occurs with dephosphorylation of S747 alone. Replacement of both S742 and S747 with glutamate gives rise to kinase- and swelling-insensitive channels that exhibit activity and biophysical properties similar to those of wild-type CLH-3b inhibited by GCK-3. Our studies provide novel insights into ClC regulation and mechanisms of cell volume signaling, and provide the foundation for studies aimed at defining how conformational changes in the cytoplasmic C terminus alter ClC gating and function in response to intracellular signaling events.

The Journal of General Physiology

INTRODUCTION

ClC genes are expressed in all phyla from bacteria to mammals. Members of the ClC superfamily of transport proteins function as anion channels or Cl^-/H^+ exchangers in plasma and intracellular organelle membranes and play key roles in diverse and fundamental physiological processes, including transepithelial Cl^- transport, organelle acidification, regulation of cytoplasmic Cl^- levels and skeletal muscle membrane excitability, and regulation of nitrate content in plants and cation homeostasis in yeast. Nine ClC genes are expressed in humans and mutations in at least four of these are associated with muscle, bone, kidney, and neurological diseases (Jentsch et al., 2002, 2005; Jentsch, 2008; Miller, 2006).

Despite intensive study and their functional importance, little is known about how ClC channels are regulated and regulatory signaling pathways have not been defined. The nematode *Caenorhabditis elegans* provides numerous experimental advantages for defining the molecular bases of fundamental physiological processes, including cellular signaling pathways (Barr, 2003; Strange, 2003). We recently demonstrated that the *C. elegans* ClC gene *clh-3* encodes two anion channel splice variants. CLH-3b is expressed in the worm oocyte and is activated during oocyte meiotic cell cycle progression, a process termed meiotic maturation, and in response to oocyte swelling (Rutledge et al., 2001; Denton et al., 2004). Meiotic maturation is the physiologically relevant stimulus for channel activation (Rutledge et al., 2001), which functions to synchronize oocyte cell cycle events with ovulation and fertilization (Rutledge et al., 2001; Strange, 2002; Yin et al., 2004).

Activation of CLH-3b in response to meiotic maturation or cell swelling occurs via serine/threonine dephosphorylation events that are mediated by the type I protein phosphatases GLC-7α and GLC-7β (Rutledge et al., 2002). Inhibition of CLH-3b is mediated by the recently identified Ste20 kinase, germinal center kinase (GCK)-3 (Denton et al., 2005). Ste20-type kinases comprise a large superfamily that is divided into p21-activated kinase and GCK subfamilies (Dan et al., 2001).

Correspondence to Kevin Strange: kevin.strange@vanderbilt.edu

Abbreviations used in this paper: GCK, germinal center kinase; KD, kinase-dead; LC-MS/MS, liquid chromatography-tandem mass spectrometry; MS, mass spectrometry.

The Rockefeller University Press $30.00
J. Gen. Physiol. Vol. 133 No. 1 29–42
www.jgp.org/cgi/doi/10.1085/jgp.200810080

Members of Ste20 superfamily regulate numerous fundamental physiological processes, including the cell cycle, apoptosis, cellular stress responses, morphogenesis, and oocyte meiotic maturation (Dan et al., 2001; Strange et al., 2006; Ling et al., 2008). GCK-3 is a homologue of mammalian SPAK and OSR1, which bind to, phosphorylate, and regulate the cell volume–sensitive activity of cation-Cl^- cotransporters (Strange et al., 2006; Delpire and Gagnon, 2008).

To determine whether CLH-3b itself is a target of regulatory phosphorylation, we performed mass spectrometric phosphopeptide analysis. GCK-3 binds to a 101–amino acid splice insert on the cytoplasmic C terminus of the channel, and binding is required for channel inhibition (Denton et al., 2005). Mass spectrometry (MS) and mutagenesis studies identified two phosphorylated serine residues downstream of the GCK-3 binding. These residues conform to the recently identified Ste20 phosphorylation motif (Zhou et al., 2004). Phosphorylation of both residues is required for channel inhibition. Our results provide novel insights into ClC regulatory signaling pathways and, along with previous studies (Denton et al., 2005; He et al., 2006), suggest structural mechanisms by which phosphorylation regulates channel activity.

MATERIALS AND METHODS

Transfection and Whole Cell Patch Clamp Recording

Human embryonic kidney (HEK293) cells were cultured in 35-mm diameter tissue culture plates in Eagle's minimal essential medium (MEM; Invitrogen) containing 10% fetal bovine serum (Hyclone Laboratories, Inc.), nonessential amino acids, sodium pyruvate, 50 U/ml penicillin, and 50 µg/ml streptomycin. After reaching 40–50% confluency, cells were transfected using FuGENE 6 (Roche) with 1 µg of green fluorescent protein (GFP), 1 µg CLH-3b, and 1 µg GCK-3 cDNAs ligated into pcDNA3.1. Point mutations in CLH-3b and GCK-3 were generated using a QuikChange Site-Directed Mutagenesis kit (Agilent Technologies). All mutants were confirmed by DNA sequencing.

After transfection, cells were incubated at 37°C for 24–30 h. Approximately 2 h before patch clamp experiments, cells were detached from growth plates by exposure to 0.25% trypsin containing 1 mM EDTA (Invitrogen) for 45 s. Detached cells were suspended in MEM, pelleted by centrifugation, resuspended in fresh MEM, and then plated onto poly-L-lysine–coated coverslips. Plated coverslips were placed in a bath chamber mounted onto the stage of an inverted microscope. Cells were visualized by fluorescence and differential interference contrast microscopy.

Transfected cells were identified by GFP fluorescence and patch clamped using a bath solution containing 90 mM NMDG-Cl, 5 mM $MgSO_4$, 1 mM $CaCl_2$, and 12 mM HEPES free acid titrated to pH 7.0 with CsOH, 8 mM Tris, 5 mM glucose, 80 mM sucrose, and 2 mM glutamine (pH 7.4, 295 mOsm), and a pipette solution containing 116 mM NMDG-Cl, 2 mM $MgSO_4$, 20 mM HEPES, 6 mM CsOH, 1 mM EGTA, 2 mM ATP, 0.5 mM GTP, and 10 mM sucrose (pH 7.2, 275 mOsm). Cells were swollen by exposure to a hypotonic (225 mOsm) bath solution that contained no added sucrose. Exposure to hypotonic solution was limited to 1 min to avoid contamination of CLH-3b current traces by activation of the ubiquitous outwardly rectifying Cl^- current $I_{Cl,swell}$ (Rutledge et al., 2002; Denton et al., 2005). Swelling-induced current amplitude was measured at −100 mV. Characterization of all mutant channels was performed on at least two independently transfected groups of cells.

Patch electrodes were pulled from 1.5-mm outer diameter–silanized borosilicate microhematocrit tubes. Electrode resistances ranged from 4 to 8 MΩ. Currents were measured with an Axopatch 200B (MDS Analytical Technologies) patch clamp amplifier. Electrical connections to the patch clamp amplifier were made using Ag/AgCl wires and 3 M KCl/agar bridges. Data acquisition and analysis were performed using pClamp 10 software (MDS Analytical Technologies).

Data Analysis

Whole cell currents were evoked by stepping membrane voltage for 1 s between −140 and +60 mV in 20-mV increments from a holding potential of 0 mV. Test pulses were followed by a 1-s interval at 0 mV. Current-to-voltage relationships were constructed from mean CLH-3b current values recorded over the last 20 msec of each test pulse.

Coexpression of CLH-3b with GCK-3 causes striking changes in channel voltage sensitivity and the kinetics of hyperpolarization-induced activation (Denton et al., 2005). Channel activation voltages were estimated from current-to-voltage relationships. A line was drawn by linear regression analysis of currents measured between 0 and 60 mV. A second line was drawn by linear regression analysis of currents measured between the first voltage at which inward current was detected and a second voltage 20 mV more negative. The intercept of these two lines is defined as the activation voltage.

The kinetics of hyperpolarization-induced channel activation are presented as 50% rise time, which is the time required for the current to reach half-maximal activation during a test pulse to −100 mV. Time constants for hyperpolarization-induced activation were also determined by fitting current traces with mono- or bi-exponential functions over the first 500 msec of test pulses after decay of the capacitance transient.

Liquid Chromatography-Tandem MS (LC-MS/MS) Analysis and Protein Identification

Chinese hamster ovary cells were cultured at 37°C in Ham's F12 medium (Invitrogen) containing 10% fetal bovine serum (Hyclone Laboratories, Inc.), 50 U/ml penicillin, and 50 µg/ml streptomycin. Cells grown in 100-mm diameter tissue culture plates to ∼50% confluency were transfected using FuGENE 6 (Roche) with 8 µg of V5-tagged CLH-3b and 3 µg of either GCK-3 or kinase-dead (KD) GCK-3 cDNAs ligated into pcDNA3.1. Approximately 28 h after transfection, 10 culture plates were rinsed twice with PBS (2.7 mM KCl, 144 mM NaCl, 1.5 mM KH_2PO_4, and 8.1 mM Na_2HPO_4, pH 7.4) and placed on ice. Cells were lysed by adding 0.4 ml of ice-cold modified RIPA lysis buffer (PBS containing 0.05% SDS and 1% Triton X-100) containing complete protease inhibitor cocktail (Roche) and 1 mM of sodium orthovandate. After 10–15 min, lysed cells were scraped, collected, passed through a 23-gauge needle, and incubated on ice for an additional 10–15 min. Lysates were centrifuged for 20 min at 10,000 *g* and 4°C, and pooled supernatants were pre-cleared with protein A/G PLUS agarose (Santa Cruz Biotechnology, Inc.). Cleared supernatants were incubated overnight with protein A/G PLUS agarose and anti-V5 antibody (Invitrogen). Immunoprecipitated proteins were washed five times with modified RIPA buffer and heated to 60°C for 40 min in NuPage LDS sample buffer (Invitrogen) containing 2 M of freshly prepared urea.

Immunoprecipitated CLH-3b protein was resolved by SDS-PAGE and digested in gel with trypsin or chymotrypsin by adaptations of standard methods (Hellman et al., 1995; Jones et al., 2003). LC-MS/MS analysis of the resulting peptides was performed using

a Thermo LTQ ion trap mass spectrometer or a Thermo LTQ-Orbitrap as described previously (Popescu et al., 2006; Lapierre et al., 2007). Dynamic exclusion settings were set for a list size of 50 and an exclusion time of 60 s with a repeat count of 1.

Samples were also analyzed in a targeted fashion in which one full MS scan from 400–2,000 m/z was acquired, followed by the acquisition of MS/MS or MS/MS/MS scans collecting MS/MS spectra for the doubly charged version of the SITHLSFGR peptide (509.27 m/z) and the corresponding mono-phosphorylated peptide (549.26 m/z) and doubly phosphorylated peptide (589.24 m/z). In addition, MS/MS/MS spectra of the neutral loss of phosphoric acid ion (that results from the phosphorylation) were targeted for the peptide with one or two phosphorylations (549.26 to 500.27 m/z; 589.24 to 540.56 m/z; 589.26 to 491.27 m/z). MS/MS and MS/MS/MS spectra were collected using an isolation width of 2 m/z for the data-dependent methods and 4 m/z for the targeted method. In these experiments, three unmodified tryptic peptides from the CLH-3b protein (KILTVEEK at 480.3 m/z, LVHGSSGGIFENESR at 794.885 m/z, and YVDSQIGTK at 505.76 m/z) were also targeted to look for relative changes in phosphorylation as described previously (Erickson et al., 2008). All methods used an activation time of 30 ms and activation Q of 0.250 and 30% normalized collision energy using 1 microscan (2 microscans for MS/MS/MS scans) and maximum injection time of 100 s for each scan on the LTQ and 500 s on the LTQ-Orbitrap. The LTQ-Orbitrap was run such that the full MS scans were collected at 60,000 resolution and AGC target value of 100,000.

Data were searched as described previously (Lapierre et al., 2007) against a FASTA database containing *C. elegans* sequences from version WS151 of the WormBase database (http://www.wormbase.org) along with the *Escherichia coli* sequences from the Uniref100 database (http://www.uniprot.org) downloaded in December 2005. The database was reversed so that false discovery rates could be determined, and the reversed version of each protein sequence was appended to the forward database for a total of 95,488 sequences. Additional analysis of MS/MS and MS/MS/MS data was performed using a P-Mod algorithm and software developed by Hansen et al. (2005). All modified spectra were manually inspected and verified.

Statistical Analyses

Data are presented as means ± SE or SD. Statistical significance was determined using Student's two-tailed *t* test for paired or unpaired means. P-values of ≤0.05 were taken to indicate statistical significance. Graphs are plotted on common scales to facilitate comparison between experimental groups.

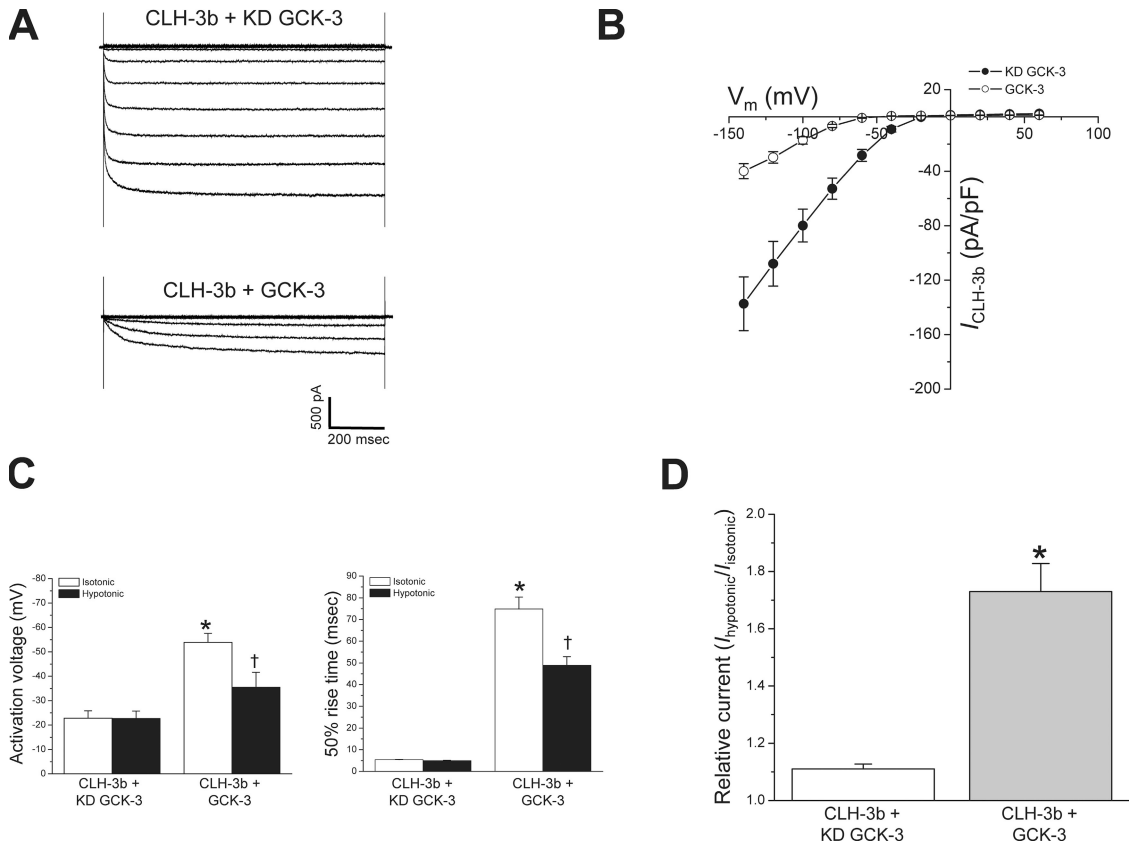

Figure 1. CLH-3b is inhibited by GCK-3. (A) Examples of whole cell currents in HEK293 cells coexpressing CLH-3b and functional or KD GCK-3. Currents were evoked by stepping membrane voltage for 1 s between −140 and +60 mV in 20-mV increments from a holding potential of 0 mV. Test pulses were followed by a 1-s interval at 0 mV. (B) Current-to-voltage relationships of CLH-3b coexpressed with functional or KD GCK-3. Coexpression of CLH-3b and GCK-3 significantly ($P < 0.001$) reduced current density over the entire range of potentials where the channels were active. Values are means ± SE ($n = 8$–12). (C) Activation voltages and 50% rise times of whole cell currents in cells coexpressing CLH-3b and KD GCK-3 or GCK-3. Values were recorded before and 1 min after exposure to a hypotonic bath. Rise times were measured after current activation at −100 mV. (D) Effect of cell swelling on current amplitude in cells coexpressing CLH-3b and KD GCK-3 or GCK-3. Currents were recorded at −100 mV before and 1 min after exposure to a hypotonic bath. Values are means ± SE ($n = 8$–12). *, $P < 0.0001$ compared with non-swollen (i.e., isotonic) cells expressing CLH-3b and KD GCK-3. †, $P < 0.005$ compared with non-swollen cells expressing CLH-3b and GCK-3.

Online Supplemental Material

Fig. S1 provides chromatograms and spectra from the targeted MS analysis of the phosphorylated SITHLSFGR peptide consistent with phosphorylation at S747 and an N-terminal residue, either S742 or T744. Fig. S2 details the data-dependent LC-MS analysis of the SITHLSFGR peptide phosphorylated at both S742 and S747. The T744A mutant exhibits wild-type channel properties, and this is illustrated in Fig. S3. To provide additional evidence that phosphorylation of both S742 and S747 is required for inhibition by GCK-3, properties of the S742A, S747E and S742E, S747A mutants are given in Fig. S4. Figs. S1–S4 are available at http://www.jgp.org/cgi/content/full/jgp.200810080/DC1.

RESULTS

GCK-3 Inhibits CLH-3b Current Amplitude and Alters Channel Gating Kinetics and Voltage Sensitivity

Fig. 1 A shows examples of whole cell current traces recorded from cells coexpressing CLH-3b and GCK-3 or control cells coexpressing the channel and a GCK-3 KD mutant. Mean current-to-voltage relationships are shown in Fig. 1 B. At all voltages where channel activity was detected, current amplitude was significantly ($P < 0.005$) greater in control cells (Fig. 1 B). Thus, as shown previously (Denton et al., 2005), GCK-3 inhibits whole cell current amplitude.

Reduced current amplitude (Fig. 1, A and B) could reflect inhibition of CLH-3b by GCK-3 or reduced membrane expression of functional channels. It must be stressed that GCK-3 induces three distinct changes in CLH-3b biophysical properties. Specifically, GCK-3 (1) induces an ∼2.4-fold hyperpolarizing shift in activation voltage from ∼−23 to ∼−54 mV (Fig. 1 C), (2) induces an ∼15-fold slowing of the 50% rise time from ∼5 to ∼75 msec (Fig. 1 C), and (3) eliminates the fast activation time constant (see Fig. 9) (Denton et al., 2005). These changes in the biophysical characteristics of the current rule out the possibility that coexpression of CLH-3b with GCK-3 simply reduces the number of functional channels. Importantly, the biophysical properties of GCK-3–inhibited CLH-3b are similar to those observed in *C. elegans* oocytes before activation of the channel by swelling or meiotic maturation (Rutledge et al., 2001, 2002).

Because CLH-3b coexpressed with KD GCK-3 is constitutively active, cell swelling has little effect on current amplitude. As shown in Fig. 1 D, the mean increase in whole cell current observed 1 min after induction of cell swelling was ∼11%. In contrast, the activity of CLH-3b coexpressed with GCK-3 was increased ∼73% by 1 min of cell swelling (Fig. 1 D). Exposure of cells to hypotonic bath for 1 min decreased the rise time significantly ($P < 0.0001$) and shifted the activation voltage to a more depolarized value ($P < 0.005$) in cells expressing GCK-3, but had no significant ($P > 0.7$) effect on these parameters in control cells (Fig. 1 C).

Data shown in Fig. 1 are consistent with our previous results (Denton et al., 2005). These findings demonstrate that (1) CLH-3b expressed in the absence of functional GCK-3 is constitutively active, (2) GCK-3 inhibits channel activity, and (3) cell swelling reverses the inhibitory effect of GCK-3. Swelling-induced reversal of inhibition is due to net dephosphorylation brought about by a decrease in GCK-3 activity and/or an increase in the activity of phosphatases (Rutledge et al., 2002).

S742 and S747 Phosphorylation Increases in the Presence of GCK-3

Fig. 2 shows a block diagram of CLH-3b intramembrane and intracellular domains. GCK-3 binds to a SPAK binding motif (Piechotta et al., 2002) located at the beginning of a 101–amino acid splice insert unique to CLH-3b, and binding is required for channel inhibition (Denton et al., 2005). This splice insert is termed a "regulatory domain."

To determine if CLH-3b is a target of regulatory phosphorylation, we performed data-dependent LC-MS/MS analysis of tryptic digests of CLH-3b immunoprecipitated from cells coexpressing GCK-3 or KD GCK-3. Initial analyses revealed that the SITHLSFGR tryptic peptide was phosphorylated at S747 as well as a site on the N terminus at S742 or T744 (Fig. S1, A–D). However, we were unable to differentiate between phosphorylation of S742 or T744 due to the lack of sufficient fragment ions to distinguish these two sites.

To further resolve phosphorylation changes at these sites, we performed an additional set of immunoprecipitation studies and targeted the singly and doubly phosphorylated SITHLSFGR peptide and three unmodified reference peptides (see Table I) for both LC-MS/MS and LC-MS/MS/MS analysis. Tryptic digests were analyzed in triplicate, and MS data were manually inspected to determine the peak areas for SITHLSFGR peptides, which were

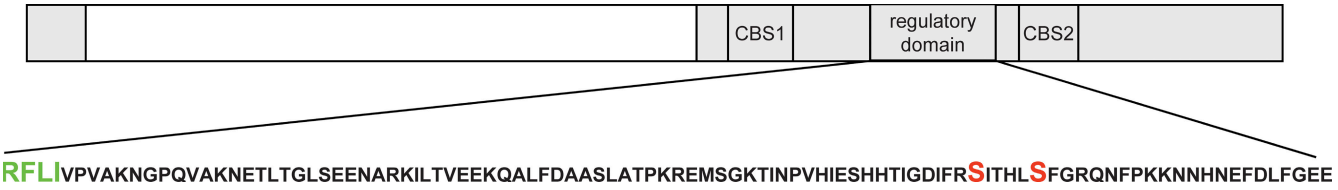

Figure 2. CLH-3b functional domains. Open and shaded bars are predicted intramembrane and intracellular domains, respectively. Relative size of domains is approximately to scale. The regulatory domain is a 101–amino acid splice insert unique to CLH-3b (Denton et al., 2004). Sequence of regulatory domain is shown. Green highlighting indicates location of GCK-3 binding site (Denton et al., 2005). Serines 742 and 747 are highlighted in red.

TABLE I

Relative Change in Phosphorylation of the SITHLSFGR Peptide in Cells Coexpressing CLH-3b and Functional GCK-3 or KD GCK-3

Peptide modification[a]	Description	Relative phosphorylation
SITHLS(-18)FGR	Single phosphorylation at S747	7.8 ± 1.8
S(80)ITHLS(80)FGR	Double phosphorylation at S742 and S747	16 ± 3

Samples of CLH-3b protein isolated from cells expressing CLH-3b in the presence of either active GCK-3 or KD GCK-3 were evaluated by targeted MS/MS analysis (see Materials and methods). Peak areas were determined for each of the modified SITHLSFGR peptides indicated and the peak areas for the unmodified reference peptides KILTVEEK, LVHGSSGGIFENESR, and YVDSQIGTK. The peak areas for the phosphorylated SITHLSFGR peptide were then normalized to the peak areas for each of the unmodified reference peptides. Relative phosphorylation was calculated as the ratio of peak areas of the SITHLSFGR peptide from cells expressing functional GCK-3 or KD GCK-3. Values are means ± SD for three separate MS runs.

[a]Phosphorylation can be identified by an increase in peptide mass of +80, which corresponds to the addition of a phosphate group (HPO_3). It can also be identified by the neutral loss of H_3PO_4 from the phosphorylated peptide. When compared to a peptide that is not phosphorylated, a net decrease in peptide mass of −18 is detected. (−18) and (80) refer to the peptide mass changes that were observed. The MS/MS/MS spectra of the neutral loss of phosphoric acid from the singly phosphorylated peptide allowed us to distinguish the phosphorylation at S747 versus S742 (see Figs. S1, B–D).

normalized to the peak areas of the three reference peptides. As shown in Table I, an approximately eightfold increase in phosphorylation at S747 was evident in cells coexpressing CLH-3b and functional GCK-3. We were also able to resolve in these studies an SITHLSFGR peptide where phosphorylation of both S742 and S747 but not T744 was evident (Fig. S2, A and B). Fig. 3 is a representative chromatogram demonstrating the increase in the normalized mass spectral signal for the doubly phosphorylated peptide in the presence of GCK-3 as compared with KD GSK-3, further demonstrating that both S742 and S747 are phosphorylated in the same peptide. Table I shows the relative changes in the abundance of the SITHLSFGR peptide phosphorylated at S747 or at both S742 and S747 in cells expressing GCK-3 as compared with KD GCK. Phosphorylation of the doubly phosphorylated peptide increased ∼16-fold in cells expressing functional GCK-3.

Phosphorylation of S747 Is Required for GCK-3–mediated Channel Inhibition

To determine whether S747 plays a role in channel regulation, we mutated it to alanine and coexpressed the

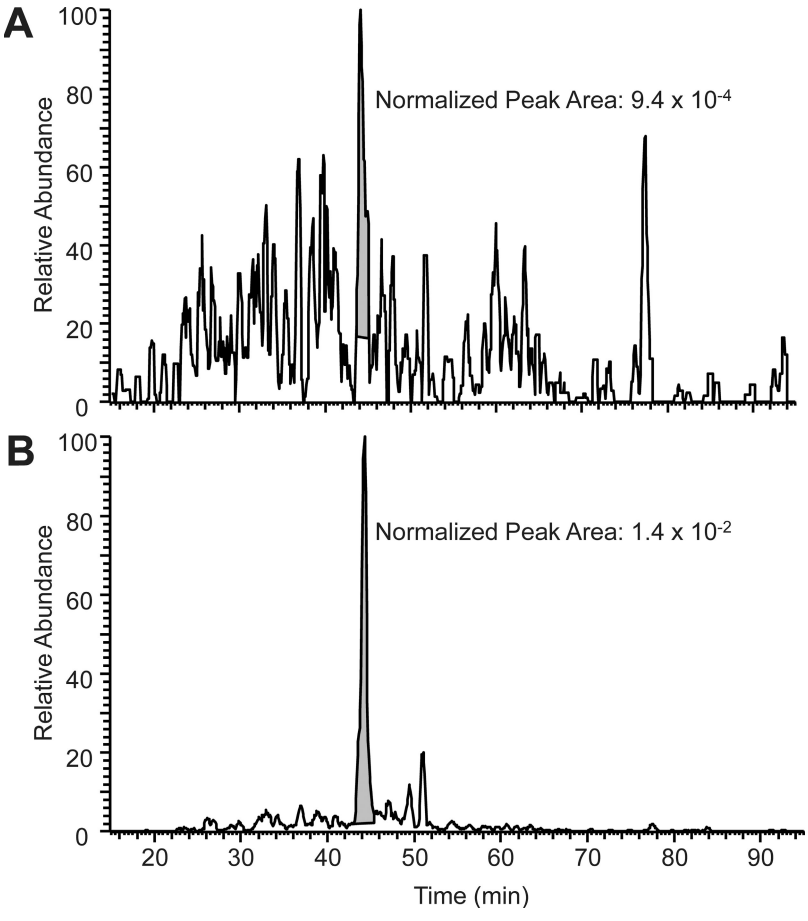

Figure 3. Representative extracted ion chromatograms from targeted MS/MS analysis of the SITHLSFGR peptide phosphorylated at both S742 and S747 in cells expressing KD GCK-3 (A) or functional GCK-3 (B). Shading shows the peak areas for the doubly phosphorylated SITHLSFGR peptide. These areas were normalized to the CLH-3b tryptic peptide KILTVEEK and are reported on each plot. In cells expressing functional GCK-3, phosphorylation of SITHLSFGR increases 15-fold. Similar fold changes were obtained in three replicate analyses and with normalization of the peak areas to two other CHL-3b tryptic peptides, LVHGSSGGIFENESR and YVDSQIGTK.

S747A mutant with active or KD GCK-3. As shown in Fig. 4 A, GCK-3 had no significant ($P > 0.5$) inhibitory effect on whole cell current amplitude. Mean activation voltages and 50% rise times (Fig. 4 B) were unaffected ($P > 0.2$) by GCK-3 or cell swelling and were not significantly ($P > 0.2$) different from those of wild-type CLH-3b coexpressed with KD GCK-3 (Fig. 4 B). Cell swelling caused a small but significantly ($P < 0.04$) greater increase in whole cell current amplitude of the S747A mutant expressed with GCK-3 versus KD GCK-3 (Fig. 4 C). However, swelling-induced activation of the S747A channel was dramatically suppressed compared with wild-type CLH-3b (Fig. 4 C), and swelling had no significant ($P > 0.2$) effect on activation voltage or rise time (Fig. 4 B). Collectively, these results indicate that the S747A mutant is constitutively active and that its activity is largely unaffected by GCK-3. Phosphorylation of S747 thus plays an important role in CLH-3b regulation.

The effects of phosphorylation on protein function can often be mimicked by replacement of phosphorylated amino acids with glutamate or aspartate residues. To further characterize the functional role of S747, we replaced it with glutamate. When coexpressed with KD GCK-3, current amplitude of the S747E mutant was similar to that of wild-type CLH-3b (Fig. 5 A). Activation voltages and 50% rise times were ~−40 mV and ~10 msec. These values were not significantly ($P > 0.9$) altered by cell swelling (Fig. 5 B).

Interestingly, when compared with wild-type CLH-3b, the S747E mutant exhibited a significant ($P < 0.05$) leftward shift in activation voltage from ~−23 to ~−40 mV in the absence of GCK-3 activity and from ~−54 to ~−72 mV when coexpressed with the functional kinase (compare Figs. 1 D and 5 B). In addition, this mutation induced a small (~50%) but significant ($P < 0.001$) increase in rise time (compare Figs. 1 D and 5 B). Results qualitatively similar to those shown in Fig. 5 were obtained using a S747D mutant where S747 was replaced with an aspartate residue (not depicted).

Collectively, the results indicate that the S747E and S747D mutants are constitutively active and suggest that aspartate or glutamate substitutions may not be effective

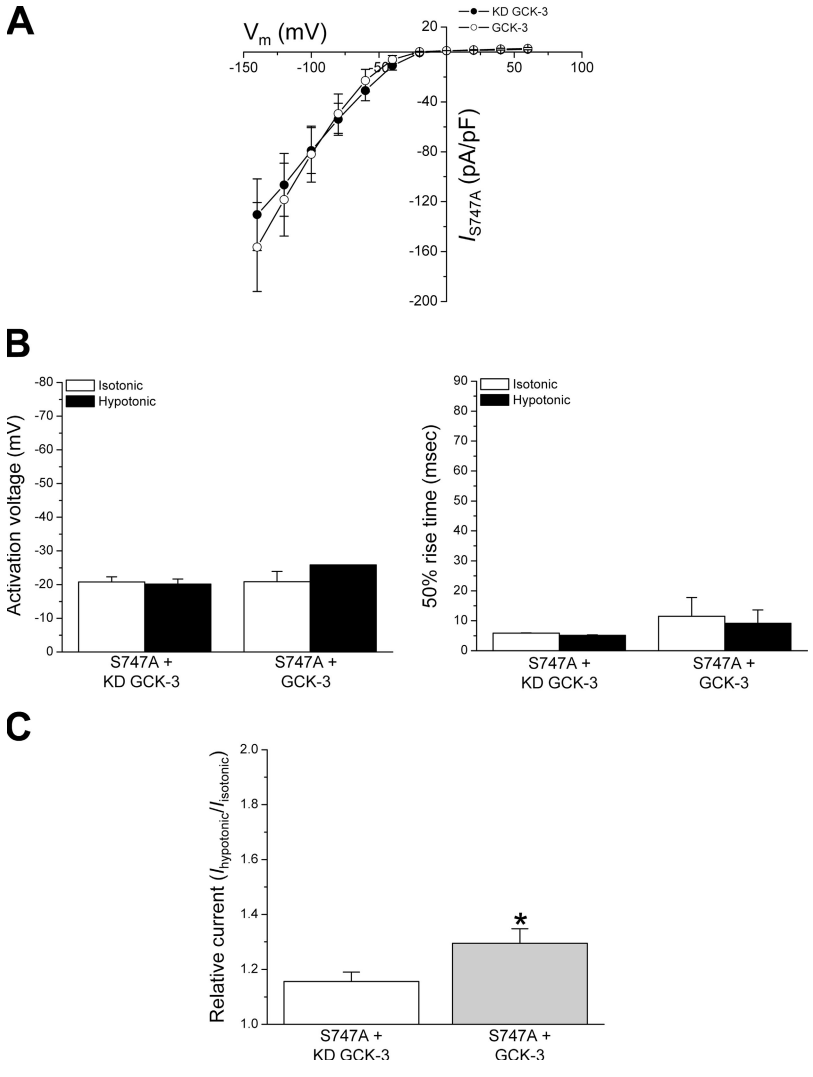

Figure 4. Mutation of S747 to alanine prevents GCK-3–mediated inhibition of CLH-3b. (A) Current-to-voltage relationships of the S747A mutant coexpressed with functional or KD GCK-3. Values are means ± SE (n = 6–9). (B) Activation voltages and 50% rise times of whole cell currents in cells coexpressing the S747A mutant and KD GCK-3 or GCK-3. Values are means ± SE (n = 6–9). (C) Effect of cell swelling on current amplitude in cells coexpressing the S747A mutant and KD GCK-3 or GCK-3. Values are means ± SE (n = 6–9). *, $P < 0.04$. Data were obtained as described in the legend to Fig. 1.

phosphoserine mimics. An alternative hypothesis is that channel inhibition requires concomitant phosphorylation of S747 and other amino acids. Data in Fig. 5 support the latter possibility. As shown in Fig. 5 (A and B), coexpression of the S747E mutant with functional GCK-3 significantly ($P < 0.02$) reduced current amplitude and significantly ($P < 0.002$) increased activation voltage and 50% rise time. These results demonstrate clearly that GCK-3 can inhibit the S747E mutant. Importantly, however, the inhibitory effects of GCK-3 on the mutant channel were not reversed by a hypotonic bath. Unlike wild-type CLH-3b (see Fig. 1), cell swelling did not significantly ($P > 0.5$) reduce activation voltage or 50% rise time (Fig. 5 B) and did not increase ($P > 0.5$) current amplitude (Fig. 5 C) of the S747E mutant coexpressed with GCK-3. The S747D mutant showed similar behavior (not depicted).

The simplest interpretation of these findings is (1) that phosphorylation of S747 and one or more additional amino acids mediate channel inhibition, and (2) that S747 and possibly other phosphorylated amino acids must be dephosphorylated during cell swelling to activate CLH-3b. Because E747 or D747 cannot be "dephosphorylated," S747E/D mutant channels coexpressed with and inhibited by GCK-3 are insensitive to cell swelling.

S742 Is a Target of GCK-3–mediated Regulatory Phosphorylation

To assess the role of S742 in channel regulation, we mutated it to alanine. As shown in Fig. 6, GCK-3 was unable to inhibit S742A mutant channels. Whole cell current amplitude, activation voltage, and 50% rise time of the S742A mutant were not significantly ($P > 0.4$) different from those of wild-type CLH-3b expressed with KD GCK-3 and were not altered significantly ($P > 0.2$) by GCK-3 under isotonic conditions and after cell swelling (Fig. 6, A–C).

To further examine the role of S742, we mutated it to glutamate. The behavior of the S742E mutant under isotonic conditions was overall similar to that of S747E channels (see Fig. 5). When coexpressed with KD GCK-3,

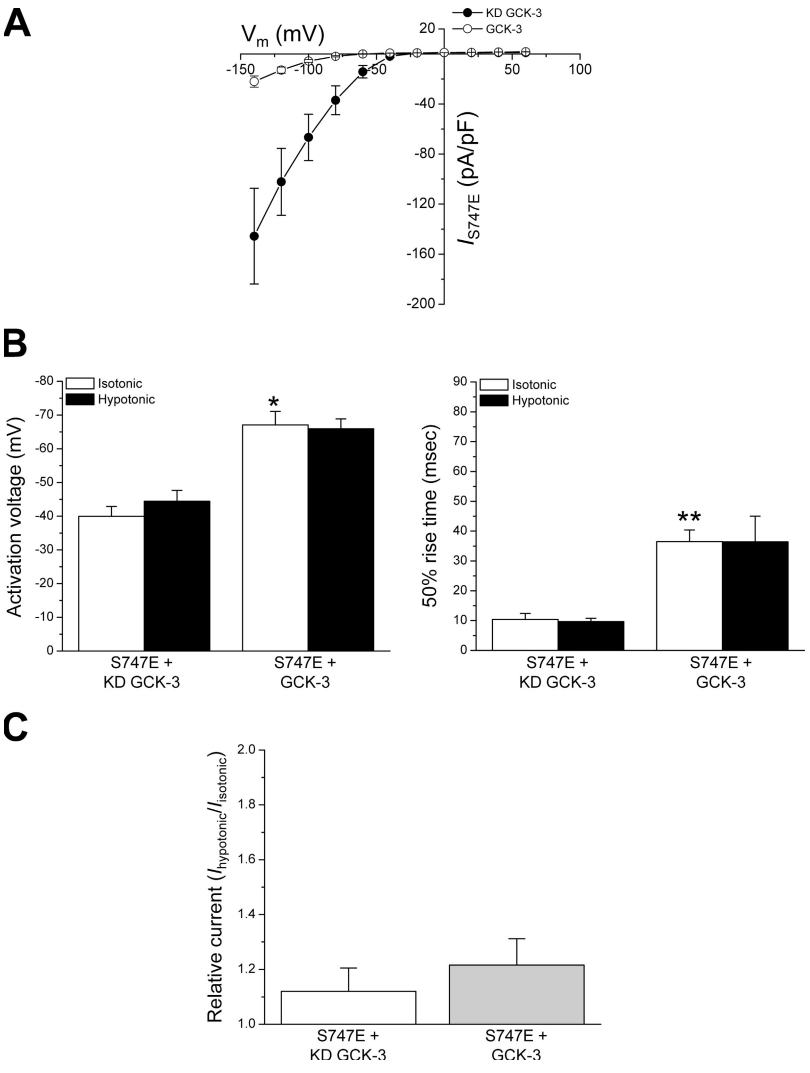

Figure 5. The CLH-3b S747E mutant is inhibited by GCK-3. (A) Current-to-voltage relationships of the S747E mutant coexpressed with functional or KD GCK-3. Coexpression of S747E with GCK-3 significantly ($P < 0.02$) reduced current density over the entire range of potentials where the channels were active. Values are means ± SE (n = 8–14). (B) Activation voltages and 50% rise times of whole cell currents in cells coexpressing the S747E mutant and KD GCK-3 or GCK-3. GCK-3 significantly ($P < 0.002$) increased activation voltage and 50% rise time. Values are means ± SE (n = 8–14). *, $P < 0.001$ and **, $P < 0.002$ compared with KD GCK-3. (C) Effect of cell swelling on current amplitude in cells coexpressing the S747E mutant and KD GCK-3 or GCK-3. Inhibition of whole cell current amplitude by GCK-3 was not altered significantly ($P > 0.1$) by cell swelling. Values are means ± SE (n = 14). Data were obtained as described in the legend to Fig. 1.

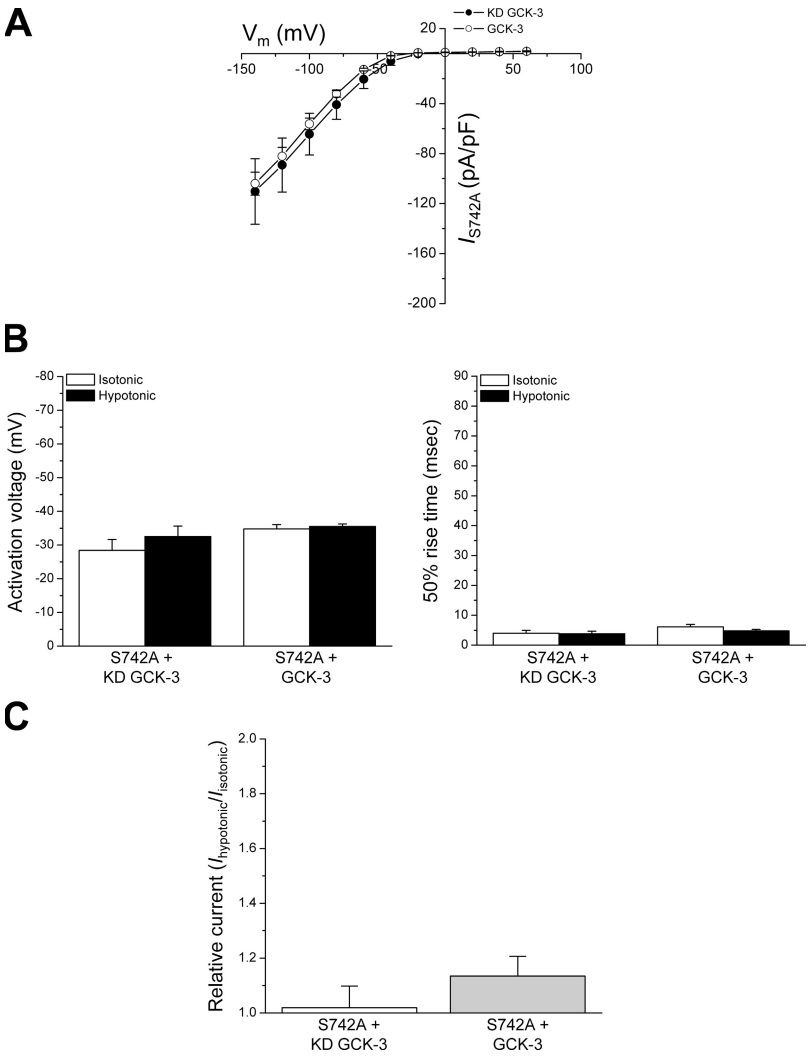

Figure 6. Mutation of S742 to alanine prevents GCK-3–mediated inhibition of CLH-3b. (A) Current-to-voltage relationships of the S742A mutant coexpressed with functional or KD GCK-3. Values are means ± SE (n = 7). (B) Activation voltages and 50% rise times of whole cell currents in cells coexpressing the S742A mutant and KD GCK-3 or GCK-3. Values are means ± SE (n = 7). (C) Effect of cell swelling on current amplitude in cells coexpressing the S742A mutant and KD GCK-3 or GCK-3. Values are means ± SE (n = 7). Data were obtained as described in the legend to Fig. 1.

current amplitude, activation voltages, and 50% rise times were not significantly ($P > 0.7$) different from those of wild-type CLH-3b. Coexpression of the S742E mutant with GCK-3 significantly ($P < 0.01$) inhibited whole cell current amplitude, increased activation voltage, and slowed activation kinetics (Fig. 7, A and B). However, unlike the S747E mutant, cell swelling increased the activity of S742E channels coexpressed with GCK-3. Whole cell current amplitude increased ~70% in cells coexpressing S742E and GCK-3 compared with ~10% in cells coexpressing S742E and KD GCK-3 ($P < 0.02$) (Fig. 7 C). Cell swelling also caused significant ($P < 0.002$) decreases in activation voltage and 50% rise times of the S742E mutant coexpressed with GCK-3 (Fig. 7 B). Similar results were observed using a S742D mutant where S742 was replaced with an aspartate residue (not depicted).

Because of initial uncertainty about whether T744 was a target of regulatory phosphorylation, we also mutated this residue to alanine. As shown in Fig. S3, the T744A mutation had no effect on channel properties or inhibition by GCK-3. These results demonstrate that T744 plays no role in GCK-3–dependent channel regulation.

GCK-3–mediated Inhibition of CLH-3b Requires Concomitant Phosphorylation of S742 and S747

Data shown in Figs. 3–7 indicate that both S742 and S747 must be phosphorylated in order for CLH-3b to be inhibited by GCK-3. Consistent with this idea, we found that GCK-3 was unable to inhibit the double-mutant channels S742A, S747E and S742E, S747A (Fig. S4). To further assess the combined role of these two amino acid residues in channel regulation, we mutated them both to glutamate. As shown in Fig. 8 A, whole cell current amplitude of the S742E, S747E mutant was dramatically reduced and was not significantly ($P > 0.2$) different from that of cells coexpressing wild-type CLH-3b and GCK-3 (see Fig. 1 B).

As noted earlier, reduction of current amplitude alone may reflect reduced membrane expression of functional CLH-3b. However, mutation of both S742 and S747 induced changes in current properties resembling those of wild-type channels coexpressed with and

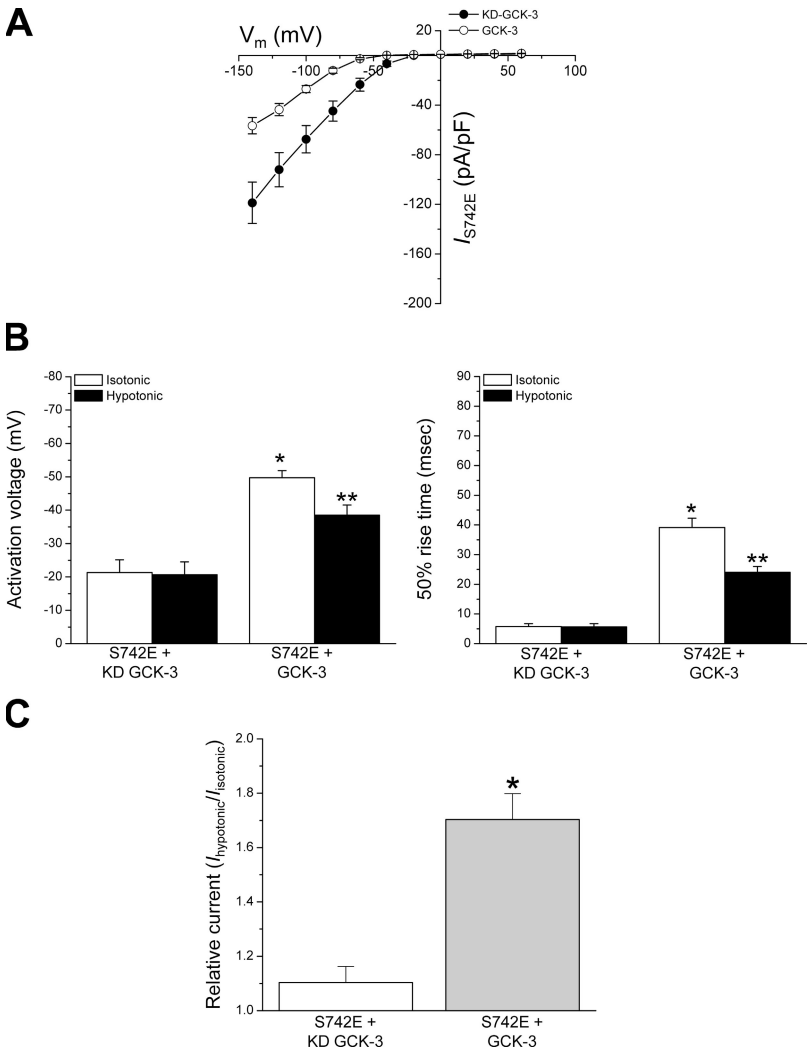

Figure 7. The CLH-3b S742E mutant is inhibited by GCK-3. (A) Current-to-voltage relationships of the S742E mutant coexpressed with functional or KD GCK-3. Coexpression of S742E with GCK-3 significantly ($P < 0.01$) reduced current density over the entire range of potentials where the channels were active. Values are means ± SE (n = 7–16). (B) Activation voltages and 50% rise times of whole cell currents in cells coexpressing the S742E mutant and KD GCK-3 or GCK-3. Values are means ± SE (n = 7–16). *, $P < 0.001$ compared with KD GCK-3 isotonic. **, $P < 0.002$ compared with GCK-3 isotonic. (C) Effect of cell swelling on current amplitude in cells coexpressing the S742E mutant and KD GCK-3 or GCK-3. Values are means ± SE (n = 16). *, $P < 0.02$. Data were obtained as described in the legend to Fig. 1.

inhibited by GCK-3. The activation voltage of the S742E, S747E mutant was hyperpolarized and 50% rise time was increased significantly ($P < 0.02$) compared with constitutively active wild-type CLH-3b coexpressed with KD GCK-3 (Fig. 8 B). Coexpression of S742E, S747E with GCK-3 had no significant ($P > 0.2$) effect on current amplitude and activation voltage, but it did cause a small (~20%; $P < 0.01$) increase in rise time (Fig. 8, A and B). None of the functional parameters of S742E, S747E channels coexpressed with either GCK-3 or KD GCK-3 were altered significantly ($P > 0.8$) by cell swelling (Fig. 8, B and C). Similar results were obtained using a S742D, S747D mutant (not depicted). Collectively, these results demonstrate that combined replacement of S742 and S747 with phosphomimetic amino acids gives rise to channels that behave as if they have been inhibited by GCK-3; S742E, S747E mutant channels show greatly reduced whole cell current amplitude, a strong hyperpolarizing shift in activation voltage, and slowed activation kinetics. S742E, S747E mutant channels cannot be dephosphorylated and therefore cannot be activated by cell swelling.

Phosphorylation Inhibits the Fast Component of Channel Gating

The kinetics of hyperpolarization-induced activation of wild-type CLH-3b expressed alone or with KD GCK-3 are well described by the sum of two exponentials that define fast and slow time constants (τ_{fast} and τ_{slow}) (Fig. 9 A) (Denton et al., 2005). In contrast, the activation kinetics of channels coexpressed with GCK-3 are described by a single time constant similar to that of τ_{slow} (Fig. 9 A). As discussed previously, these results suggest that GCK-3 may inhibit a fast gating process (Denton et al., 2005).

We derived time constants for voltage-dependent activation of all mutant channels. As expected, the activation kinetics of mutants that were inhibited by GCK-3 were defined by a single slow time constant when they were coexpressed with the kinase. Similarly, the activation kinetics of mutant channels that were unaffected by GCK-3 were described by fast and slow time constants in the presence and absence of functional kinase (not depicted). Importantly, the activation kinetics of S742E, S747E mutant channels were described by a single slow time constant when they were expressed with either KD

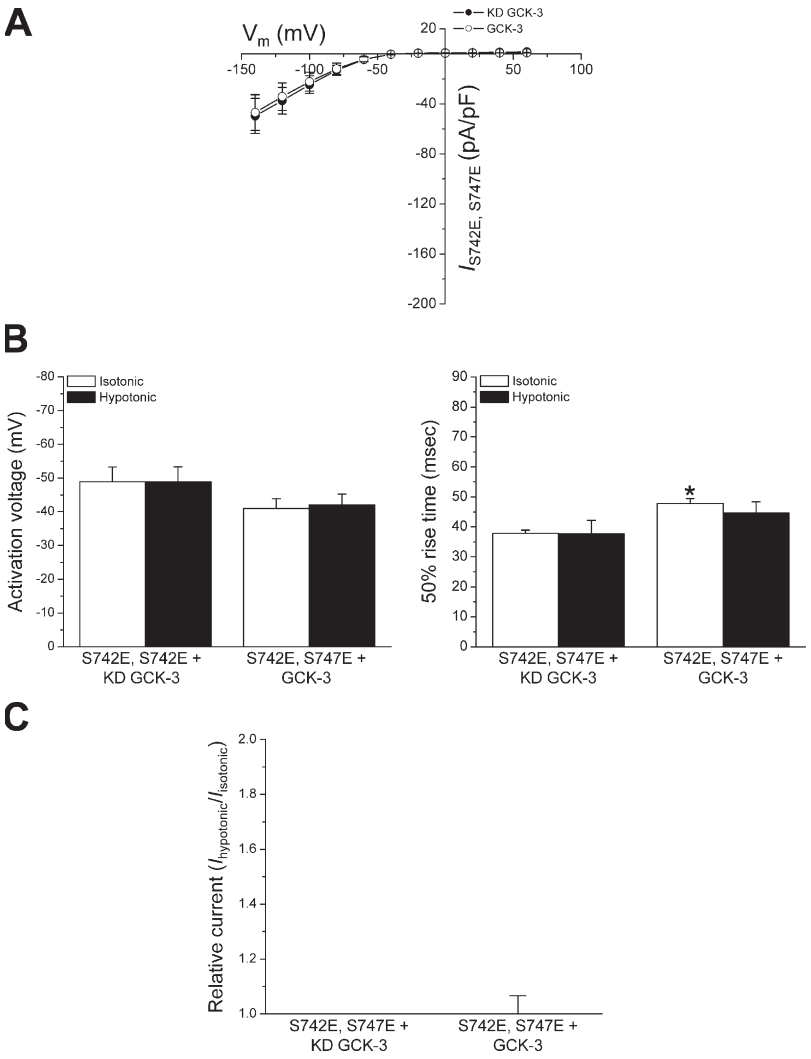

Figure 8. CLH-3b S74E, S747E mutant channels are constitutively inhibited and unaffected by GCK-3. (A) Current-to-voltage relationships of the S742E, S747E double mutant coexpressed with functional or KD GCK-3. Values are means ± SE ($n = 6–7$). (B) Activation voltages and 50% rise times of whole cell currents in cells coexpressing S742E, S747E and KD GCK-3 or GCK-3. Values are means ± SE ($n = 6–7$). *, $P < 0.01$ compared with KD GCK-3 isotonic. (C) Effect of cell swelling on current amplitude in cells coexpressing S742E, S747E and KD GCK-3 or GCK-3. Values are means ± SE ($n = 6–7$). Data were obtained as described in the legend to Fig. 1.

GCK-3 or functional GCK-3 (Fig. 9 B). These results further support our conclusion that the S742E, S747E mutant behaves like wild-type CLH-3b that has been inhibited by GCK-3.

DISCUSSION

Changes in phosphorylation have been shown to regulate the activity of various ClC anion transport proteins. However, the physiological context under which such regulation occurs and the signaling cascades that mediate phosphorylation are poorly understood. In addition, phosphorylation has been shown to have opposing effects on ClCs under different experimental conditions. For example, swelling-induced activation of rat ClC-2 is inhibited by the type I protein phosphatase inhibitor calyculin A, suggesting that dephosphorylation activates the channel (Rutledge et al., 2002). In contrast, PKA-mediated phosphorylation activates a rabbit ClC-2 splice variant (Malinowska et al., 1995), but has no effect on rat ClC-2 (Park et al., 2001).

ClC-3 belongs to a subfamily of ClC transport proteins that function in intracellular membranes as electrogenic Cl^-/H^+ exchangers (Chen and Hwang, 2008). However, several groups have shown that heterologous expression of ClC-3 induces outwardly rectifying anion currents that are modulated by phosphorylation. As with ClC-2, phosphorylation has different effects under different experimental conditions. For example, Cl^- currents induced by expression of human ClC-3 can be activated by intracellular dialysis with autonomously active calcium/calmodulin-dependent protein kinase II (Huang et al., 2001; Robinson et al., 2004). In contrast, Cl^- currents observed in cells transfected with guinea pig ClC-3 are inhibited by phosphorylation mediated by PKA or PKC (Duan et al., 1999; Nagasaki et al., 2000). It is unclear if the varying effects of phosphorylation on ClC activity reflect species differences and/or differences in experimental conditions.

We have exploited the genetically tractable model organism *C. elegans* to characterize the physiological roles and regulatory mechanisms of ClC channels. *clh-3* and

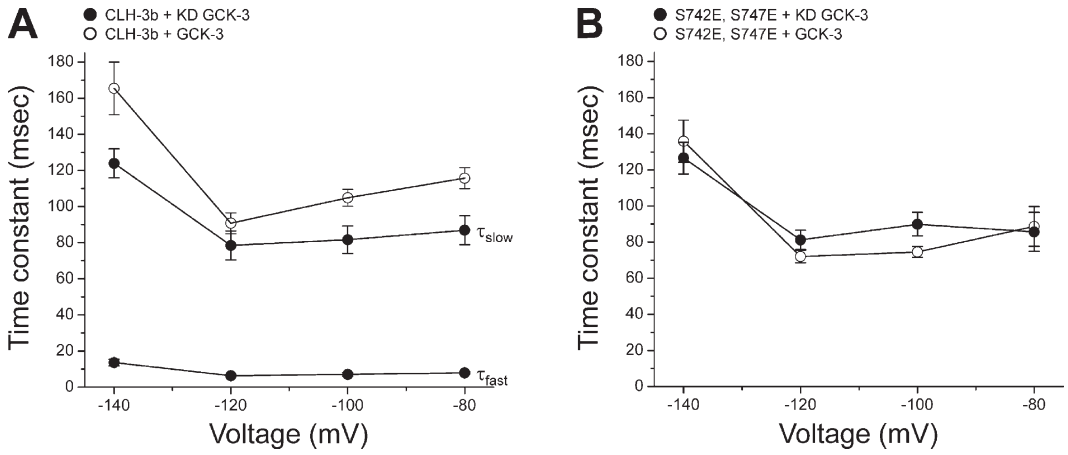

Figure 9. Phosphorylation of CLH-3b alters the kinetics of hyperpolarization-induced channel activation. Time constants describing activation kinetics of CLH-3b (A) and the S742E, S747E mutant channel (B) in response to hyperpolarizing voltage steps. Wild-type and mutant channels were coexpressed with KD or functional GCK-3. Values are means ± SE (n = 7–12).

gck-3 are coexpressed in the worm oocyte as well as the excretory cell (Schriever et al., 1999; Nehrke et al., 2000; Denton et al., 2005; Hisamoto et al., 2008). RNA interference knockdown of *gck-3* in *C. elegans* oocytes constitutively activates CLH-3b current (Denton et al., 2005). In the excretory cell, genetic analysis suggests that GCK-3 regulates excretory canal development via inhibition of *clh-3*–encoded channels (Hisamoto et al., 2008).

GCK-3 is an ortholog of mammalian SPAK and OSR1 (Choe and Strange, 2007). These kinases bind to K-Cl (KCC) and Na-K-2Cl (NKCC) cotransporters and phosphorylate them in response to cell volume changes (Delpire and Gagnon, 2008). The regulation of CLH-3b is analogous to that of the K-Cl contransporter, which is dephosphorylated and activated during cell swelling by serine/threonine phosphatases (Gamba, 2005). Recent studies by Gagnon et al. (2006) suggest that KCC2 is inhibited by SPAK-mediated phosphorylation.

GCK-3 binds to a SPAK binding motif (Piechotta et al., 2002) at the beginning of the 101–amino acid CLH-3b regulatory domain (Fig. 2). Binding is required for GCK-3 to inhibit channel activity (Denton et al., 2005). Ste20 kinases phosphorylate at serine and threonine residues that are followed in the +1 position by hydrophobic amino acids (Songyang et al., 1994; Zhou et al., 2004). S742 and S747 are located 70 and 75 amino acids downstream from the GCK-3 binding site and are followed by hydrophobic isoleucine and phenylalanine residues, respectively (Fig. 2). These findings as well as studies of cation-Cl^- cotransporter regulation by SPAK and OSR1 (Delpire and Gagnon, 2008) suggest that GCK-3 directly phosphorylates CLH-3b. However, a direct test of this hypothesis requires in vitro phosphorylation assays.

Both S742 and S747 must be phosphorylated to inhibit CLH-3b. Replacement of either of these serines with alanine prevents channel inhibition. When S742 and S747 are replaced individually with a glutamate residue, the mutant channels are constitutively active and remain sensitive to GCK-3 (Figs. 5 and 7). S742A, S747E and S742E, S747A mutants are also constitutively active but are unaffected by coexpression with the kinase (Fig. S4). Replacement of both serines with glutamate gives rise to kinase and swelling-insensitive channels that exhibit activity and biophysical properties similar to those of wild-type CLH-3b coexpressed with GCK-3 (Figs. 8 and 9).

The requirement that both S742 and S747 be phosphorylated for inhibition of CLH-3b has important implications for channel regulation. Multisite phosphorylation has been observed with numerous proteins and can occur in either a processive or nonprocessive (i.e., distributive) manner (Patwardhan and Miller, 2007). With processive phosphorylation, the kinase binds and sequentially phosphorylates all target amino acids before unbinding. Distributive phosphorylation involves repeated cycles of kinase binding, phosphorylation, and unbinding to fully phosphorylate the protein. Processive phosphorylation is efficient, allowing full modulation of protein function each time an activated kinase binds. A distributive mechanism decreases the likelihood of spurious phosphorylation and associated changes in protein activity. In addition, the rate of substrate phosphorylation in a distributive process is sensitive to the concentration of activated kinase. Small changes in kinase activity can thus have a large effect on the rate of phosphorylation and subsequent changes in the activity of the target protein (Patwardhan and Miller, 2007).

Little is known about the mechanisms by which cells sense volume perturbations. However, these mechanisms are exquisitely sensitive. For example, studies by Lohr and Grantham (1986) on the renal proximal tubule and Kuang et al. (2006) on cultured corneal endothelial cells have demonstrated that cells can sense and respond to volume changes induced by osmotic perturbations of only 2–3 milliosmoles. Phosphorylation of volume-sensitive

channels and cation-Cl^- cotransporters via a distributive mechanism may contribute to this sensitivity.

It is presently unclear whether changes in swelling-induced dephosphorylation and activation of CLH-3b are brought about by reductions in GCK-3 activity and/or increases in the activity of phosphatases. Indirect evidence from studies of cation-Cl^- cotransporters suggests that they are regulated by a volume-sensitive kinase that operates in the presence of constant and unregulated phosphatase activity (Jennings and al-Rohil, 1990; Lytle, 1998; Jennings, 1999). Thus, increases or decreases in kinase activity brought about by cell volume perturbations induce concomitant increases or decreases in cotransporter phosphorylation. It remains to be determined whether GCK-3 and/or other kinases are the volume-sensitive components of the CLH-3b regulatory pathway.

Interestingly, activation of CLH-3b in response to cell swelling occurs with dephosphorylation of S747 alone. S747E mutant channels coexpressed with GCK-3 are not activated by cell volume increase (Fig. 5). In contrast, S742E channels inhibited by GCK-3 exhibit swelling-induced increases in current amplitude and decreases in activation voltage and rise time comparable to that of wild-type CLH-3b (compare Figs. 1, C and D, and 7, B and C). These results suggest two possibilities. First, swelling-induced dephosphorylation of the channel may be an ordered process requiring S747 to be dephosphorylated before S742. Partial dephosphorylation may in turn allow partial activation of CLH-3b in response to different levels or types of stimuli. Alternatively, the phosphorylation of S742 may simply be a permissive event required for protein conformational changes to take place in response to phosphorylation and dephosphorylation of S747 that in turn inhibit or activate CLH-3b. Unfortunately, these possibilities cannot be tested using mammalian expression systems. Mammalian cells express an outwardly rectifying anion current, $I_{Cl,\ swell}$, that is activated dramatically by cell swelling (Hartzell et al., 2008). The presence of this current limits the amount of time cells can be swelled and therefore prevents assessment of the full degree to which wild-type and mutant CLH-3b channels can be activated. Alternative expression systems may be useful for assessing how dephosphorylation regulates channel function.

ClC channels are homodimers, and each monomer forms a pore that is independently gated by a so-called "fast" gate that opens and closes on a millisecond timescale. A "common" gate with much slower kinetics closes both pores simultaneously (Miller, 2006; Jentsch, 2008). The kinetics of hyperpolarization-induced activation of wild-type CLH-3b expressed in the absence of functional GCK-3 are described by the fast and slow time constants (Fig. 9 A) (Denton et al., 2005). Voltage-dependent activation of CLH-3b is described by a single slow time constant when the channel is inhibited by GCK-3 or by mutation of both S742 and S747 to glutamate (Fig. 9) (Denton et al., 2005). As we have proposed previously (Denton et al., 2005), this suggests indirectly that phosphorylation may inhibit the fast gating mechanism.

Deletion of the CLH-3b regulatory domain gives rise to channels with voltage sensitivity and kinetics of hyperpolarization-induced activation that resemble those of wild-type channels coexpressed with GCK-3 (He et al., 2006). It is interesting to speculate that the CLH-3b regulatory domain may interact with other parts of the channel. Phosphorylation of S742 and S747 could disrupt this interaction leading to channel inhibition. Deletion of the entire regulatory domain would also disrupt protein–protein interactions and mimic phosphorylation.

How could changes in the conformation of the cytoplasmic C terminus lead to changes in channel gating? ClC proteins are comprised of 18 α-helical domains (designated "A-R"), 17 of which are membrane embedded (Dutzler et al., 2002, 2003). The R-helix forms part of the channel pore and selectivity filter (Dutzler et al., 2002, 2003). In eukaryotic ClC proteins, the R-helix connects via a short linker to a large cytoplasmic C terminus. Dutzler et al. (2002) proposed that this linker may provide a pathway by which conformational changes in the cytoplasmic C terminus could be transmitted to the intramembrane domain and thereby alter channel gating and pore properties. Recent studies on ClC-1 (Hebeisen and Fahlke, 2005), CLH-3b (He et al., 2006), and ClC-Kb (Martinez and Maduke, 2008) have demonstrated that C terminus mutations give rise to extracellular structure/function changes. Clearly though, extensive additional studies will be required to define how phosphorylation events alter cytoplasmic C terminus conformation and how those conformational changes in turn regulate CLH-3b gating.

This work was supported by National Institutes of Health (NIH) R01 grants DK51610 and DK61168 to K. Strange and NIH training grants 5T32 NS007491-07 and 5F32 DK080576-02 to R.A. Falin. Experiments described in this paper were proposed and designed by R.A. Falin, R. Morrison, A.-J.L. Ham, and K. Strange. Experimental procedures were carried out by R.A. Falin, R. Morrison, and A.-J.L. Ham. All authors participated in the analysis and interpretation of data, in the writing of the manuscript, and in the approval of the final version of the manuscript for publication.

Edward N. Pugh Jr. served as editor.

Submitted: 17 July 2008
Accepted: 17 November 2008

REFERENCES

Barr, M.M. 2003. Super models. *Physiol. Genomics.* 13:15–24.

Chen, T.Y., and T.C. Hwang. 2008. CLC-0 and CFTR: chloride channels evolved from transporters. *Physiol. Rev.* 88:351–387.

Choe, K.P., and K. Strange. 2007. Evolutionarily conserved WNK and Ste20 kinases are essential for acute volume recovery and survival following hypertonic shrinkage in *Caenorhabditis elegans*. *Am. J. Physiol.* 293:C915–C927.

Dan, I., N.M. Watanabe, and A. Kusumi. 2001. The Ste20 group kinases as regulators of MAP kinase cascades. *Trends Cell Biol.* 11:220–230.

Delpire, E., and K.B. Gagnon. 2008. SPAK and OSR1: STE20 kinases involved in the regulation of ion homoeostasis and volume control in mammalian cells. *Biochem. J.* 409:321–331.

Denton, J., K. Nehrke, E. Rutledge, R. Morrison, and K. Strange. 2004. Alternative splicing of N- and C-termini of a *C. elegans* ClC channel alters gating and sensitivity to external Cl^- and H^+. *J. Physiol.* 555:97–114.

Denton, J., K. Nehrke, X. Yin, R. Morrison, and K. Strange. 2005. GCK-3, a newly identified Ste20 kinase, binds to and regulates the activity of a cell cycle–dependent ClC anion channel. *J. Gen. Physiol.* 125:113–125.

Duan, D., S. Cowley, B. Horowitz, and J.R. Hume. 1999. A serine residue in ClC-3 links phosphorylation-dephosphorylation to chloride channel regulation by cell volume. *J. Gen. Physiol.* 113:57–70.

Dutzler, R., E.B. Campbell, M. Cadene, B.T. Chait, and R. MacKinnon. 2002. X-ray structure of a ClC chloride channel at 3.0 A reveals the molecular basis of anion selectivity. *Nature.* 415:287–294.

Dutzler, R., E.B. Campbell, and R. MacKinnon. 2003. Gating the selectivity filter in ClC chloride channels. *Science.* 300:108–112.

Erickson, J.R., M.L. Joiner, X. Guan, W. Kutschke, J. Yang, C.V. Oddis, R.K. Bartlett, J.S. Lowe, S.E. O'Donnell, N. Aykin-Burns, et al. 2008. A dynamic pathway for calcium-independent activation of CaMKII by methionine oxidation. *Cell.* 133:462–474.

Gagnon, K.B., R. England, and E. Delpire. 2006. Volume sensitivity of cation-Cl- cotransporters is modulated by the interaction of two kinases: Ste20-related proline-alanine-rich kinase and WNK4. *Am. J. Physiol.* 290:C134–C142.

Gamba, G. 2005. Molecular physiology and pathophysiology of electroneutral cation-chloride cotransporters. *Physiol. Rev.* 85:423–493.

Hansen, B.T., S.W. Davey, A.J.L. Ham, and D.C. Liebler. 2005. P-Mod: an algorithm and software to map modifications to peptide sequences from tandem MS data. *J. Proteome Res.* 4:358–368.

Hartzell, H.C., Z. Qu, K. Yu, Q. Xiao, and L.T. Chien. 2008. Molecular physiology of bestrophins: multifunctional membrane proteins linked to best disease and other retinopathies. *Physiol. Rev.* 88:639–672.

He, L., J. Denton, K. Nehrke, and K. Strange. 2006. Carboxy terminus splice variation alters ClC channel gating and extracellular cysteine reactivity. *Biophys. J.* 90:3570–3581.

Hebeisen, S., and C. Fahlke. 2005. Carboxy-terminal truncations modify the outer pore vestibule of muscle chloride channels. *Biophys. J.* 89:1710–1720.

Hellman, U., C. Wernstedt, J. Gonez, and C.H. Heldin. 1995. Improvement of an "In-Gel" digestion procedure for the micropreparation of internal protein fragments for amino acid sequencing. *Anal. Biochem.* 224:451–455.

Hisamoto, N., T. Moriguchi, S. Urushiyama, S. Mitani, H. Shibuya, and K. Matsumoto. 2008. *Caenorhabditis elegans* WNK-STE20 pathway regulates tube formation by modulating ClC channel activity. *EMBO Rep.* 9:70–75.

Huang, P., J. Liu, A. Di, N.C. Robinson, M.W. Musch, M.A. Kaetzel, and D.J. Nelson. 2001. Regulation of human CLC-3 channels by multifunctional Ca^{2+}/calmodulin-dependent protein kinase. *J. Biol. Chem.* 276:20093–20100.

Jennings, M.L. 1999. Volume-sensitive K^+/Cl^- cotransport in rabbit erythrocytes. Analysis of the rate-limiting activation and inactivation events. *J. Gen. Physiol.* 114:743–758.

Jennings, M.L., and N. al-Rohil. 1990. Kinetics of activation and inactivation of swelling-stimulated K^+/Cl^- transport. The volume-sensitive parameter is the rate constant for inactivation. *J. Gen. Physiol.* 95:1021–1040.

Jentsch, T.J. 2008. CLC chloride channels and transporters: from genes to protein structure, pathology and physiology. *Crit. Rev. Biochem. Mol. Biol.* 43:3–36.

Jentsch, T.J., V. Stein, F. Weinreich, and A.A. Zdebik. 2002. Molecular structure and physiological function of chloride channels. *Physiol. Rev.* 82:503–568.

Jentsch, T.J., M. Poet, J.C. Fuhrmann, and A.A. Zdebik. 2005. Physiological functions of CLC Cl^- channels gleaned from human genetic disease and mouse models. *Annu. Rev. Physiol.* 67:779–807.

Jones, J.A., L. Kaphalia, M. Treinen-Moslen, and D.C. Liebler. 2003. Proteomic characterization of metabolites, protein adducts, and biliary proteins in rats exposed to 1,1-dichloroethylene or diclofenac. *Chem. Res. Toxicol.* 16:1306–1317.

Kuang, K., M. Yiming, Z. Zhu, P. Iserovich, F.P. Diecke, and J. Fischbarg. 2006. Lack of threshold for anisotonic cell volume regulation. *J. Membr. Biol.* 211:27–33.

Lapierre, L.A., K.M. Avant, C.M. Caldwell, A.J. Ham, S. Hill, J.A. Williams, A.J. Smolka, and J.R. Goldenring. 2007. Characterization of immunoisolated human gastric parietal cells tubulovesicles: identification of regulators of apical recycling. *Am. J. Physiol.* 292:G1249–G1262.

Ling, P., T.J. Lu, C.J. Yuan, and M.D. Lai. 2008. Biosignaling of mammalian Ste20-related kinases. *Cell. Signal.* 20:1237–1247.

Lohr, J.W., and J.J. Grantham. 1986. Isovolumetric regulation of isolated S_2 proximal tubules in anisotonic media. *J. Clin. Invest.* 78:1165–1172.

Lytle, C. 1998. A volume-sensitive protein kinase regulates the Na-K-2Cl cotransporter in duck red blood cells. *Am. J. Physiol.* 274:C1002–C1010.

Malinowska, D.H., E.Y. Kupert, A. Bahinski, A.M. Sherry, and J. Cuppoletti. 1995. Cloning, functional expression, and characterization of a PKA-activated gastric Cl^- channel. *Am. J. Physiol.* 268:C191–C200.

Martinez, G.Q., and M. Maduke. 2008. A cytoplasmic domain mutation in ClC-Kb affects long-distance communication across the membrane. *PLoS ONE.* 3:e2746.

Miller, C. 2006. ClC chloride channels viewed through a transporter lens. *Nature.* 440:484–489.

Nagasaki, M., L. Ye, D. Duan, B. Horowitz, and J.R. Hume. 2000. Intracellular cyclic AMP inhibits native and recombinant volume-regulated chloride channels from mammalian heart. *J. Physiol.* 523:705–717.

Nehrke, K., T. Begenisich, J. Pilato, and J.E. Melvin. 2000. *C. elegans* ClC-type chloride channels: novel variants and functional expression. *Am. J. Physiol.* 279:C2052–C2066.

Park, K., T. Begenisich, and J.E. Melvin. 2001. Protein kinase A activation phosphorylates the rat ClC-2 Cl- channel but does not change activity. *J. Membr. Biol.* 182:31–37.

Patwardhan, P., and W.T. Miller. 2007. Processive phosphorylation: mechanism and biological importance. *Cell. Signal.* 19:2218–2226.

Piechotta, K., J. Lu, and E. Delpire. 2002. Cation chloride cotransporters interact with the stress-related kinases Ste20-related proline-alanine-rich kinase (SPAK) and oxidative stress response 1 (OSR1). *J. Biol. Chem.* 277:50812–50819.

Popescu, D.C., A.J. Ham, and B.H. Shieh. 2006. Scaffolding protein INAD regulates deactivation of vision by promoting phosphorylation of transient receptor potential by eye protein kinase C in Drosophila. *J. Neurosci.* 26:8570–8577.

Robinson, N.C., P. Huang, M.A. Kaetzel, F.S. Lamb, and D.J. Nelson. 2004. Identification of an N-terminal amino acid of the CLC-3 chloride channel critical in phosphorylation-dependent activation of a CaMKII-activated chloride current. *J. Physiol.* 556:353–368.

Rutledge, E., L. Bianchi, M. Christensen, C. Boehmer, R. Morrison, A. Broslat, A.M. Beld, A. George, D. Greenstein, and K. Strange. 2001. CLH-3, a ClC-2 anion channel ortholog activated during meiotic maturation in *C. elegans* oocytes. *Curr. Biol.* 11:161–170.

Rutledge, E., J. Denton, and K. Strange. 2002. Cell cycle- and swelling-induced activation of a *C. elegans* ClC channel is mediated by CeGLC-7α/β phosphatases. *J. Cell Biol.* 158:435–444.

Schriever, A.M., T. Friedrich, M. Pusch, and T.J. Jentsch. 1999. CLC chloride channels in *Caenorhabditis elegans*. *J. Biol. Chem.* 274:34238–34244.

Songyang, Z., S. Blechner, N. Hoagland, M.F. Hoekstra, H. Piwnica-Worms, and L.C. Cantley. 1994. Use of an oriented peptide library to determine the optimal substrates of protein kinases. *Curr. Biol.* 4:973–982.

Strange, K. 2002. Of mice and worms: novel insights into ClC-2 anion channel physiology. *News Physiol. Sci.* 17:11–16.

Strange, K. 2003. From genes to integrative physiology: ion channel and transporter biology in *Caenorhabditis elegans*. *Physiol. Rev.* 83:377–415.

Strange, K., J. Denton, and K. Nehrke. 2006. Ste20-type kinases: evolutionarily conserved regulators of ion transport and cell volume. *Physiology (Bethesda)*. 21:61–68.

Yin, X., N.J. Gower, H.A. Baylis, and K. Strange. 2004. Inositol 1,4,5-trisphosphate signaling regulates rhythmic contractile activity of smooth muscle-like sheath cells in the nematode *Caenorhabditis elegans*. *Mol. Biol. Cell.* 15:3938–3949.

Zhou, T., M. Raman, Y. Gao, S. Earnest, Z. Chen, M. Machius, M.H. Cobb, and E.J. Goldsmith. 2004. Crystal structure of the TAO2 kinase domain: activation and specificity of a Ste20p MAP3K. *Structure.* 12:1891–1900.